# 3D simulation using the lattice Boltzmann method of heat transfer in a local with different door positions

*Karim* Choukrallah[1*], *Noureddine* Abouricha[1], *Mounia* Achak[1] and *Mustapha* El Alami[2]

[1]LabSIPE, National School of Applied Sciences of El Jadida, Chouaib Doukkali University, El Jadida, Morocco
[2]LPMAT Laboratory, Physics Department, Faculty of Sciences Ain Chock, Hassan II University, Casablanca, Morocco

**Abstract.** This study numerically examines three-dimensional natural convection in a bottom-heated, closed cubic cavity using the lattice Boltzmann method. The computational approach relies on a D3Q15 lattice scheme coupled with a single-time relaxation (SRT) collision operator. The cavity's lateral and top walls are treated as adiabatic surfaces, while two specific areas on the front wall, representing a window and a door, are treated as cold regions. Simulations are performed for a Rayleigh number of $10^7$ and a Prandtl number of 0.71. Key results include the time evolution of the temperature field, temperature profiles along the x, y, and z axes, three-dimensional velocity vector maps, calculations of the local and mean Nusselt numbers on the heated surface, and graphical representations of isothermal contours on different cross-sectional planes. This research provides a robust dataset for the study of three-dimensional natural convection phenomena in a fully enclosed structure with bottom heating.

**Keywords**: LBM, 3D simulation, Natural convection, building, cubic enclosure.

## 1 Introduction

Numerical modeling of natural convection using the lattice Boltzmann method (LBM) has been extensively explored over the past decades due to its efficiency, parallel scalability, and suitability for complex geometries. Several studies have focused on coupling LBM with advanced numerical techniques to address radiative heat transfer, topology optimization, grid refinement, and multiphase thermal flows. For example, Several studies by Abouricha and co-authors [1–3] have addressed natural convection in air-filled enclosures using the Lattice Boltzmann Method. In particular, they showed that variable bottom heating with a sinusoidal temperature profile significantly affects the thermal behavior inside a square cavity, leading to higher temperature fluctuations at the cavity core, while the global Nusselt number remains weakly sensitive to the heating period [1]. Their work was later extended through combined experimental measurements and numerical simulations in a locally bottom-heated insulated enclosure, where a very good agreement between experimental data and two-dimensional LBM predictions was reported, with temperature differences not exceeding ±1 °C [2]. More recently, turbulent natural convection at high Rayleigh numbers was investigated numerically, demonstrating the strong influence of both the Rayleigh number and the size of the heat source on flow structures, temperature fields, and average heat transfer rates [3]

* Corresponding author: karimchoukrallah@gmail.com

Ben Salah et al. [4] analyzed the interaction between thermal radiation and natural convection in enclosures filled with participating media by combining LBM with the control volume finite element method (CVFEM). Cette étude met en lumière les progrès réalisés dans le cadre des approches hybrides LB–CVFEM, qui ont prouvé leur efficacité pour capturer des structures d'écoulement complexes et des effets radiatifs avec des besoins de calcul réduits. En complément, Luo et al. [5] ont développé un double MRT-LBM intégré à une méthode level-set pour l'optimisation topologique thermique tridimensionnelle. Leur approche a permis des calculs stables à des nombres de Grashof élevés, aboutissant à des conceptions efficaces de dissipateurs thermiques. De manière similaire, Xu et al. [6] ont proposé un LBM amélioré par interpolation, capable de fonctionner sur des maillages non uniformes, atteignant une précision accrue dans la convection à haut nombre de Rayleigh, notamment près des frontières. Leur méthode a démontré des performances élevées constantes tout en approchant une précision globale du troisième ordre grâce à un streaming basé sur l'interpolation. Dans le domaine des écoulements thermiques multiphasiques, Wu et al. [7] ont exploré la convection de Rayleigh–Bénard chargée de particules en utilisant un LBM thermique à double fonction de distribution, modélisant avec succès les interactions fluide-particules et l'impact des particules de taille finie sur le transfert de chaleur. En élargissant les applications pratiques, Tighchi et al. [8] ont employé une formulation LBM complète pour étudier la convection naturelle et le rayonnement volumétrique dans des matériaux à changement de phase assistés par nanofluides, élucidant le rôle des paramètres de rayonnement et de la concentration de nanoparticules dans la dynamique de fusion. Plus récemment, Channouf et al. [9] ont fusionné le MRT-LBM avec des schémas aux différences finies de Runge–Kutta pour analyser le transfert de chaleur conjugué dans des cavités contenant des corps solides de conductivité variable, révélant des changements significatifs dans les motifs d'écoulement et un transfert de chaleur accru à des nombres de Rayleigh élevés. Malgré ces avancées, les recherches restent largement concentrées sur des configurations simplifiées telles que des cavités chauffées différentiellement, des systèmes de Rayleigh–Bénard, des modèles de transfert de chaleur conjugué ou des cavités orientées vers l'optimisation. Les études portant sur la convection naturelle dans des espaces architecturaux tridimensionnels réalistes, comme des pièces équipées d'ouvertures telles que des portes ou des fenêtres, sont rares, en particulier dans des conditions de nombres de Rayleigh élevés et pour de l'air avec un nombre de Prandtl de 0,71. De plus, peu d'investigations ont utilisé le modèle LBM D3Q15 pour analyser la dynamique transitoire de l'écoulement d'air et du transfert de chaleur dans des scénarios de bâtiments contextuellement pertinents. Pour combler ces lacunes, cette étude se concentre sur la convection naturelle tridimensionnelle de l'air dans une pièce cubique comportant à la fois une porte et une fenêtre. En utilisant un cadre LBM D3Q15, des simulations ont été réalisées à un nombre de Rayleigh élevé ($Ra = 10^7$) pour explorer l'évolution temporelle des champs de vitesse, des distributions de température et du comportement global du transfert de chaleur exprimé par le nombre de Nusselt. L'objectif est de fournir des aperçus physiques plus approfondis sur les performances thermiques des bâtiments, la circulation de l'air intérieur et les techniques de ventilation passive. En abordant des défis peu explorés de la physique du bâtiment, cette recherche contribue à l'avancement des méthodologies de modélisation numérique dans le contexte d'environnements architecturaux réalistes. Modèle mathématiquePhysical Problem

The considered configuration is a cubic enclosure containing a door and a window, while all the remaining walls of the cavity are assumed to be adiabatic (Fig. 1). The enclosure is filled with air, modeled as an incompressible Newtonian fluid with a Prandtl number of Pr=0.71.

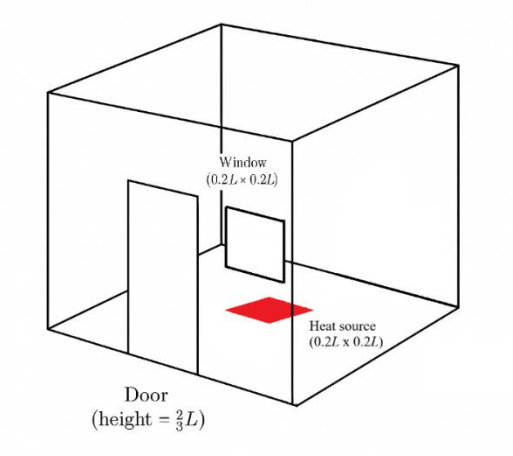


**Fig. 1.** Physical configuration

### 1.1 Governing equations

The Lattice Boltzmann Method (LBM) is a mesoscopic computational approach derived from the discretization of the Boltzmann equation in kinetic theory. It operates between the microscopic molecular dynamics and macroscopic continuum scales, modeling fluid behavior through the statistical mechanics of particle distribution functions. As with conventional computational fluid dynamics (CFD) methods, it solves the discrete governing equations on a spatially and temporally discretized lattice [10]. The hydrodynamic and thermal fields are resolved using two separate distribution functions, denoted as $f_k(\mathrm{x},t)$ and $g_k(\mathrm{x},t)$, respectively. In this work, the three-dimensional D3Q15 model is implemented on a uniform cubic lattice with unit spacing ($\Delta x = \Delta y = \Delta z = 1$) and fifteen discrete velocity vectors.

The discrete ck velocities of the D3Q15 model are defined as follows:

$$\mathrm{c_k} = \begin{pmatrix} 0 & 1 & -1 & 0 & 0 & 0 & 0 & 1 & -1 & 1 & -1 & 1 & -1 & -1 & 1 \\ 0 & 0 & 0 & 1 & -1 & 0 & 0 & 1 & -1 & 1 & -1 & -1 & 1 & 1 & -1 \\ 0 & 0 & 0 & 0 & 0 & 1 & -1 & 1 & -1 & -1 & 1 & 1 & -1 & 1 & -1 \end{pmatrix} \quad (1)$$

**For the dynamic field**

$$f(X + c_k\Delta t, t + \Delta t) = f_k(X,t) + w_m\left[f_k^{eq}(X,t) - f_k(X,t)\right] + \Delta t f_k \quad (2)$$

$w_m = \frac{\Delta t}{\tau_m}$ , $\tau_m$is the relaxation time for dynamic field and $\Delta t$=1 is the time step

**For the thermal field**

$$g(X + c_k\Delta t, t + \Delta t) = g_k(X,t) + w_s\left[g_k^{eq}(X,t) - g_k(X,t)\right] \quad (3)$$

$w_s = \frac{\Delta t}{\tau_s}$ , $\tau_s$ is the relexation time

This study enables the connection between the Boltzmann transport equation and the Navier-Stokes equations through the Chapman-Enskog expansion. It facilitates the bridging of the macroscopic and microscopic scales by elucidating the relationship between the kinematic viscosity ($\nu$)

$$\nu = c_s^2(\tau_m - \frac{1}{2}) \qquad (4)$$

Likewise for thermal diffusivity :

$$\alpha = c_s^2(\tau_s - \frac{1}{2}) \qquad (5)$$

$c_s = \frac{c}{\sqrt{3}}$ Is the lattice speed of sound

$f_k^{eq}$ And $g_k^{eq}$ are respectively the local equilibrium distribution functions for dynamic and thermal fields from where

$$f_k^{eq}(X,t) = \omega_k \rho(X,t)\left[1 + 3\frac{\vec{c_k}\vec{u}}{c^2} + \frac{9}{2}\frac{(\vec{c_k}\vec{u})^2}{c^4} - \frac{3}{2}\frac{\vec{u}\vec{u}}{c^2}\right] \qquad (6)$$

$$g_k^{eq}(X,t) = \omega_k \theta(X,t)\left[1 + 3\frac{\vec{c_k}\vec{u}}{c^2}\right] \qquad (7)$$

With $\omega_k$ referred to as nodal weights or weight factors, for D3Q15 model, are represented as follows :

$$\omega_k = \begin{pmatrix} w_0 = \frac{2}{9} \\ w_{1,\dots,6} = \frac{1}{9} \\ w_{7,\dots,14} = \frac{1}{72} \end{pmatrix} \qquad (8)$$

The boussinesq approximation is applied to the buoyancy force term the external force $F_K$ in Eq 2 is expressed as :

$$F_K = \frac{3\omega_K \rho g \beta \Delta\theta c_{K,y}}{c_s^2} \qquad (9)$$

And finally, the macroscopic quantities such as density, velocities, and temperature are computed in the following manner :

$$\rho(X,t) = \sum_{K=0}^{K=14} f_K(X,t) \qquad (10)$$

$$\rho\vec{u}\,(X,t) = \sum_{K=0}^{K=14} \vec{c_k} f_K(X,t) \qquad (11)$$

$$\theta(X,t) = \sum_{K=0}^{K=14} g_K(X,t) \qquad (12)$$

**Boundary conditions :**

- Dynamic boundary conditions for Dynamic field :

For x=0, x=1 and $0 \le y \le 1$, $0 \le z \le 1$ U=V=W=0
For y=0, x=1 and $0 \le x \le 1$, $0 \le z \le 1$ U=V=W=0
For z=0, x=1 and $0 \le x \le 1$, $0 \le y \le 1$ U=V=W=0

- Bounce-back conditions :

$$f_k(X,t) = f_{opp(K)}(X,t) \qquad (13)$$

Where : $k$ =1,2,3,4,5,6,7,8,9,10,11,12,13,14 and $opp(k)$=2,1,4,3,6,5,8,7,10,9,12,11,14,13

- Thermal boundary conditions for thermal field :

on the heat source : $\theta = \theta_h = 1$, on the door and the window: $\theta = \theta_c = 0$

**Bounce-back conditions :**

$$g_k(X,t) = \left(w_k + w_{opp(K)}\right)\theta(X,t) - g_{opp(K)}(X,t) \qquad (14)$$

- On the adiabatic walls : $\frac{\partial\theta}{\partial n} = 0$ with $n$ is the normal of walls

### 1.2 Average Nusselt number

The 3D average Nusselt number $\overline{\mathrm{N}}_{\mathrm{u3D}}$ was determined by integrating the local Nusselt number along the hot wall :

$$\overline{\mathrm{N}}_{\mathrm{u3D}} = \int_0^1 \int_0^1 \frac{\partial\theta(\mathrm{y,z})}{\partial \mathrm{x}}\Big|_{\mathrm{x=L}} \mathrm{dy\,dx} \qquad (15)$$

## 2 Validation:

The validation of our program code is done with a configuration of a cubic enclosure differentially heated and filled with air. The Table 1 presented a comparison of maximum dimensionless velocity along the horizontal centerline and hot wall average Nusselt numbers for two and three dimensions. We compared our results of the maximum dimensionless velocity along the horizontal centerline and the 2-D average Nusselt number with the corresponding results of De Vahl Davis [11]. We noticed that for all the Rayleigh numbers, the maximum dimensionless velocity comparison indicated a good agreement for all Rayleigh numbers and varied between 2.2% and 3.59%. And for the two dimensions average Nusselt number we noticed also an acceptable deviation for all values of Rayleigh numbers. For the three dimensions average Nusselt number, we compared our results with the corresponding results of Peng Wang et al, [12], and as we observed for the two dimensions average Nusselt number we noticed also an acceptable deviation also for the 3D average Nusselt number [13].

**Table 1.** Comparison of maximum dimensionless velocity along the horizontal centerline and hot wall average Nusselt numbers for 2D and 3D dimensions [13]

| | $10^3$ | $10^6$ |
|---|---|---|
| Nusselt Average 3D | 1.10 | 8.10 |
| Peng Wang [9] | 1.08 | 8.77 |
| Deviation (%) | 1,85 | 7.63 |

## 3 Results and Discussion

In this section, we present the results obtained and their analysis, highlighting the main trends, interpretation in the context of the study, and discussed the scientific significations of the numerical results.

### 3.1 Isotherms

The figure 2 (right) shows the structure of Isothermal lines for the middle door configuration, the isotherms highlight a natural convection regime dominated by Archimedes' thrust inside the cubic cavity. Near the heat source located on the lower wall, the isotherms are tightly packed, reflecting the existence of high thermal gradients and the formation of a thin thermal boundary layer. As they rise in the cavity, the isotherms gradually deform upwards, indicating vertical heat transport by convection. The relatively even distribution of isotherms in the central region suggests a well-established convective flow, characteristic of a high Rayleigh number ($Ra=10^7$). The figure 3 (left) shows the structure forme of isothermal lines for the side door configuration, the isothermal lines show a clearly asymmetrical thermal distribution inside the cubic cavity, a direct consequence of the lateral displacement of the cold door on the front wall. Around the heat source, high temperature isotherms are highly concentrated. This indicates: very high thermal gradients, a thin thermal boundary layer, and intense buoyancy generation. The thermal plume from this source is not perfectly vertical,it is gradually deflected by the thermal asymmetry imposed by the side door.

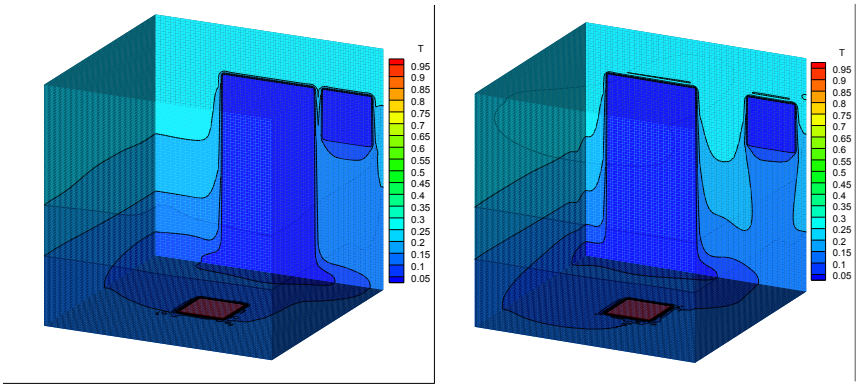


**Fig. 2.** Isothermal lines of the middle door (right) of the side door (left)

### 3.2 Temperature variation

The dimensionless temperature profiles along the z-axis highlight the impact of the heat source on natural convection heat transfer for $Ra=10^7$ (figure 3). In the both configurations the dimensionless temperature distributions decreases until the position z=0.1 approximately, and increases linearly in the intervalle of z-axis 0.1 to 1. Very high temperature near the center-bottom, indicating the presence of an internal hot zone representing an upward plume issuing from the heat source at the bottom, which maintains a high temperature at the center of the enclosure before being evacuated toward the cold door and window. Near the center-top, the temperature rises gradually to values close to 0.2–0.3. This indicates a recirculation of the fluid that heats the intermediate parts of the middle. Comparing the two curves for the two configurations, we observe that near the bottom of the cube, the curve corresponding to the middle door seems to have a slightly different initial slope compared to the side door configuration, the difference is small but noticeable this indicates a small change in the intensity of heat deposition at the ceiling depending on the position of the cold front surface. In the upper middle of the cube, the side-door configuration curve may show a slightly higher temperature (less symmetrical

plume), suggesting that the side door promotes local heat conservation and less symmetrical evacuation. This structure is characteristic of natural convection flows with a high Rayleigh number, where inertial effects become significant and lead to partial thermal stratification. Figure 4 shows the evolution of the temperature at the center of the room as a function of the number of iterations for the middle door and side door configurations. This figure demonstrates that a steady state has been established and that the temperature value at the center changes with each change in the door position.

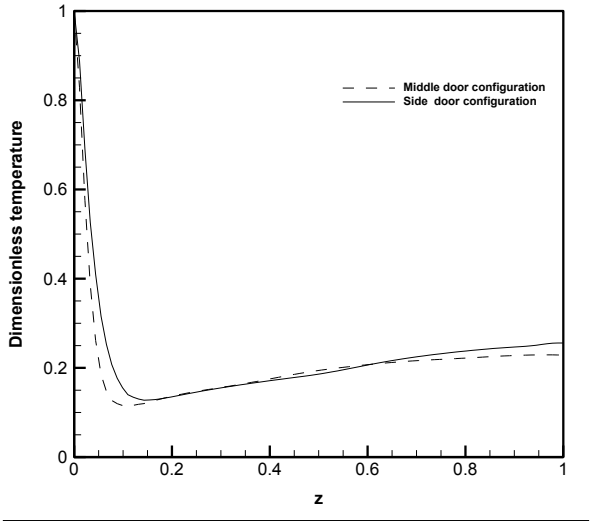


**Fig. 3.** Dimensionless **t**emperature along z-axis

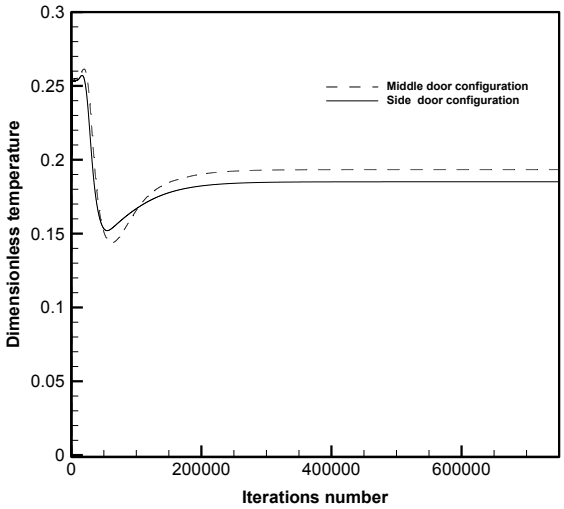


**Fig. 4.** Dimensionless temperature distribution as a function of time

### 3.3 Average Nusselt number

The table 2 indicated the Average Nusselt number values for the two configurations, middle door and side door. It can be observed that the average Nusselt number for the middle door configuration is lower than for the side door configuration, which implies that heat transfer is less significant, leading to more efficient heat accumulation compared to the side door configuration.

**Table 2.** Average Nusselt number

| Configurations | Average Nusselt number |
|---|---|
| Middle door configuration | 1.1086 |
| Side door configuration | 1.1501 |

## 4 Conclusion

In this paper, we have provided a numerical simulation and comparison of two different door position configurations using the lattice Boltzmann method in a three-dimensional cubic cavity. The results show that:

The configuration with a middle door produces organized convection with low heat transfer in the cubic cavity, which promotes significant heat accumulation in the cubic cavity compared to the configuration with a side door and provides good heating of the cubic cavity.

In general, the position of the door has a significant impact on natural convection and thermal management. For the middle door configuration, heat accumulation is greater, leading to a higher average temperature, and for the side door configuration, heat dissipation is greater and the configuration is more effective for passive cooling applications.

## References

1. ABOURICHA, Noureddine, ENNAWAOUI, Chouaib et EL ALAMI, Mustapha. Effet de l'amplitude et de la période sur le transfert de chaleur dans une enceinte chauffée par le bas de manière sinusoïdale : étude par la méthode de Boltzmann sur réseau. *Frontiers in Heat and Mass Transfer* , 2023, vol. 21, p. 523-537.
2. NOUREDDINE, Abouricha et MUSTAPHA, El Alami. Effet de la taille de la source de chaleur sur le transfert de chaleur dans un milieu chauffé localement par le bas à nombre de Rayleigh élevé. Dans : *AIP Conference Proceedings* . AIP Publishing LLC, 2021. p. 020042.
3. ABOURICHA, Noureddine, GOUNNI, Ayoub, et EL ALAMI, Mustapha. Experimental Study of Heat Transfer in an Insulated Local Heated from Below and Comparison with Simulation by Lattice Boltzmann Method. *Frontiers in Heat and Mass Transfer*, 2024, vol. 22, no 1, p. 359-375.
4. SALAH, Mohieddine Ben, MSADDAK, Ayoub, ALQAHTANI, Talal, *et al.* Prediction of volumetric radiation effect on natural convection with high Rayleigh number using lattice Boltzmann-control volume finite element method. *Case Studies in Thermal Engineering*, 2025, vol. 74, p. 106785.
5. LUO, Ji-Wang, CHEN, Li, KE, Hanbing, *et al.* Three-dimensional topology optimization of natural convection using double multiple-relaxation-time lattice Boltzmann method. *Applied Thermal Engineering*, 2024, vol. 236, p. 121732.

6. XU, Ao, ZHAO, Zheng, XU, Ben-Rui, *et al.* Interpolation-supplemented lattice Boltzmann simulation of thermal convection on non-uniform meshes. *International Journal of Heat and Mass Transfer*, 2026, vol. 255, p. 127790.
7. WU, Hongcheng, KARZHAUBAYEV, Kairzhan, SHEN, Jie, *et al.* Direct numerical simulation of three-dimensional particle-laden thermal convection using the Lattice Boltzmann Method. *Computers & Fluids*, 2024, vol. 276, p. 106268.
8. TIGHCHI, Hashem Ahmadi, SOBHANI, Masoud, et ESFAHANI, Javad Abolfazli. Nouveau stockage de chaleur latente via rayonnement volumétrique et convection naturelle nanofluidique : une étude sur treillis Boltzmann. *Journal du stockage d'énergie* , 2025, vol. 120, p. 116414.
9. CHANNOUF, Salaheddine, BENHAMOU, Jaouad et JAMI, Mohammed. Étude du transfert de chaleur par convection et conduction dans des corps chauffés carrés et circulaires : une approche novatrice utilisant la méthode couplée de Runge-Kutta et de Boltzmann sur réseau. *Thermal Science and Engineering Progress* , 2024, vol. 49, p. 102441.
10. ABOURICHA, Noureddine, EL ALAMI, Mustapha, KRIRAA, Mounir, et al. Lattice boltzmann method for natural convection flows in a full scale cavity heated from Below. Am. J. Heat Mass Transfer, 4.2 (2017): 121-135
11. DE VAHL DAVIS, G. Natural convection of air in a square cavity: a bench mark numerical solution. International Journal for numerical methods in fluids, 3.3 (1983): 249-264
12. WANG, Peng, ZHANG, Yonghao, et GUO, Zhaoli. Numerical study of three-dimensional natural convection in a cubical cavity at high Rayleigh numbers. International Journal of Heat and Mass Transfer, 113 (2017): 217-228.
13. CHOUKRALLAH, Karim, ABOURICHA, Noureddine, ACHAK, Mounia, et al. Validation of Lattice Boltzmann Method in Two and Three Dimensions. In : Defect and Diffusion Forum. Trans Tech Publications Ltd, 2026. p. 25-33.